Modeling and experimental investigation of dynamics of two pendulums elastically coupled and driven by magnetic field

Krystian Polczyński, Grzegorz Wasilewski, Jan Awrejcewicz, Adam Wijata

Abstract: In this work both experimental and simulation results of a study of two physical pendulums coupled through an elastic torsional element are presented. Permanent magnets are attached to the pendulums ends and the system motion is forced by a variable magnetic field with a help of the exciting coils. The electric current signal possesses rectangular shape, and the experimental investigations have been carried out for different frequencies and amplitudes of the current signal (excitation). The derived mathematical model has been validated experimentally taking into account its experimentally confirmed parameters. The magnetic fields interactions have been reduced to the moment of a force based on the experimentally obtained data. A few of the dynamically different cases are studied including the elastically coupled/un-coupled pendulums and the system excitation carried out either by one or two pendulums. Regular and chaotic dynamics of this mechatronic system have been detected, illustrated and discussed.

1. Introduction

In classical mechanics a pendulum (physical or mathematical) is one of the simplest objects of one-degree-of-freedom system, whose motion is governed by a nonlinear differential equation. Technical progress and combination of different branches of technologies yielded possibilities for searching new methods of driving for mechanical systems, and the magnetic forces have recently attracted interest for their employment as the sources for mechanical/mechatronical excitations. It is well known and documented that even simple pendula driven by magnetic field may exhibit a rich dynamic behavior including periodic motions [1], parametric and self-excited oscillations [2], numerous parametric resonances [3], and chaotic behaviors [1, 3, 4].

In a series of papers [1-4] the magnetic field interaction has been simplified to the Gilbert model of magnetic dipole [5]. However, in contrary to the latter investigations the magnetic interaction in our work is expressed as mathematical function based on experimental data, in contrary to the mentioned theoretical model.

2. Experimental rig and electric excitation signal

Fig. 1 presents the setup of the constructed experimental stand. The test stand is equipped with two pendulums marked as (1) and (2). The pendulums are attached to the axes (3) which are hold by rolling bearings. The axes are joined with a cuboid elastic element (4) made of rubber. Pendulum (2)

always has a neodymium magnet (5) (not visible) at the end of the rod. In the case of the pendulum (1), the neodymium magnet can be replaced by a brass element with the same dimensions and mass as the mentioned magnet. Air-core coils (6) (0.022 H inductance) are located below the pendulums. Distance between the coil and the magnet during our experiment was equal to h=0.0016 m (it is possible to regulate this distance). On the axes are also attached wheels (7) used for measurement of static characteristics of the moment of force, that comes from the magnetic interaction. The experimental rig is made of non-magnetic materials like brass, aluminum or polymer composites to reduce its influence on the activated magnetic fields.

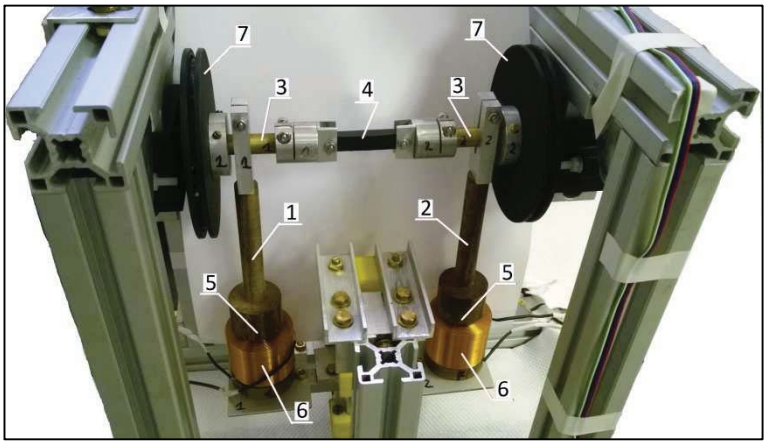

Figure 1. Experimental rig (1 – pendulum, 2 – pendulum, 3 – axis, 4 – elastic element, 5 – neodymium magnet, 6 – air-core coil, 7 – wheel).

Fig. 2 shows a shape of the electric current signal which flows through the coils. The signal can flow through one coil or two coils at the same time. The frequency $\left(f = \frac{1}{\tau}\right)$, duty cycle $\left(w = \frac{\tau_z}{\tau} \cdot 100\%\right)$ and amplitude are controlled. The I_{1a}, I_{2a} denote the amplitudes of the current, where I_{1a} and I_{2a} stand for the pendulum 1 and the pendulum 2, respectively.

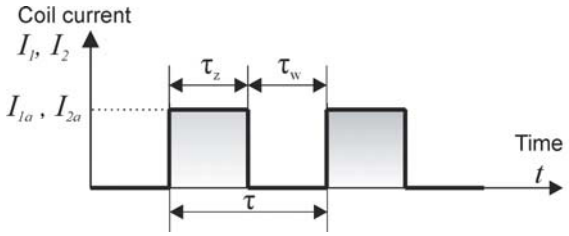

Figure 2. Excitation current signal (τ_z – current ON; τ_w – current OFF; $\tau = \tau_z + \tau_w$ – period; $w = \frac{\tau_z}{\tau} \cdot 100\%$ - duty cycle).

3. Mathematical model

This section describes the mathematical model of the experimental rig presented in section 2. The physical model of the experimental rig is shown in Fig. 3.

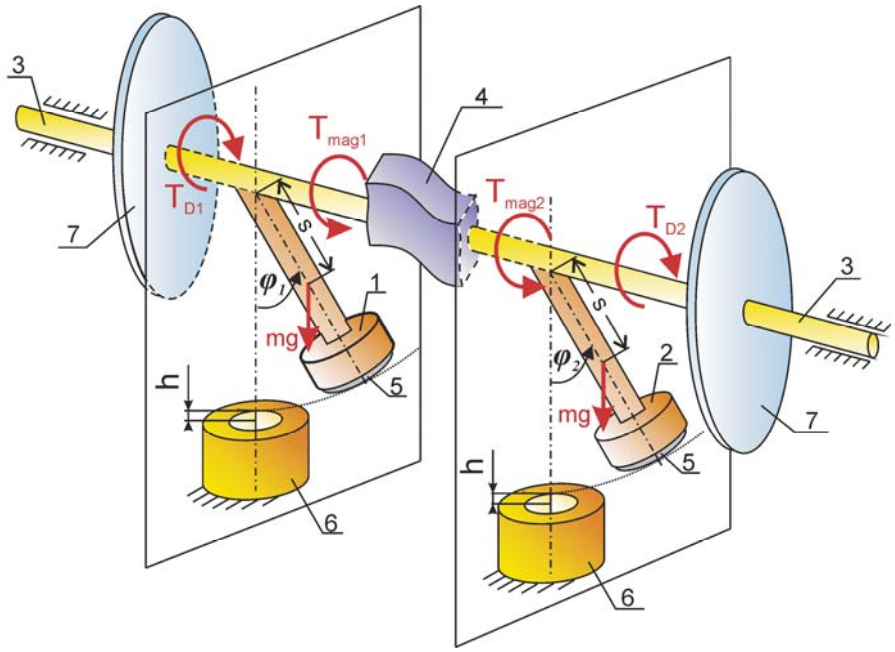

Figure 3. Physical model of the experimental stand.

The mathematical model is created accordingly to the laws of the classical mechanics. It has been developed considering the four torques acting on the each pendulum. General equations of motion of the pendulums are as follows

$$I_1\ddot{\varphi}_1 = T_{mag1} - T_{D1} - mgs \cdot \sin\varphi_1 - k_e(\varphi_1 - \varphi_2), \tag{1}$$

$$I_2\ddot{\varphi}_2 = T_{mag2} - T_{D2} - mgs \cdot \sin\varphi_2 - k_e(\varphi_2 - \varphi_1), \tag{2}$$

where: I_1, I_2 – moments of inertia of the pendulums, T_{mag1}, T_{mag2} – magnetic interaction torques, T_{D1}, T_{D2} – damping torques, mg – weight of the pendulum, s – length between center of mass of the pendulum and the axis of rotation, $k_e(\varphi_1 - \varphi_2)$ – torsional deformation torque of elastic element, where k_e is a stiffness of the element.

Torques T_{D1} and T_{D2} are sum of all damping factors which act on the pendulums during their motions, i.e. we have the

$$T_{D1} = c_1\dot{\varphi}_1 + c_e(\dot{\varphi}_1 - \dot{\varphi}_2) + c_{B1} \cdot sgn(\dot{\varphi}_1)\ ,$$

$$T_{D2} = c_2\dot{\varphi}_2 + c_e(\dot{\varphi}_2 - \dot{\varphi}_1) + c_{B2} \cdot sgn(\dot{\varphi}_2)\ , \tag{3}$$

where: $c_1\dot{\varphi}_1, c_2\dot{\varphi}_2$ – the viscous torques, $c_e(\dot{\varphi}_1 - \dot{\varphi}_2)$, $c_e(\dot{\varphi}_2 - \dot{\varphi}_1)$ are the damping torques of the elastic element, $c_{B1} \cdot sgn(\dot{\varphi}_1), c_{B2} \cdot sgn(\dot{\varphi}_2)$ – friction torques of the bearings ($c_1, c_2, c_e, c_{B1}, c_{B2}$ are constant coefficients).

Torques T_{mag1} and T_{mag2} define the magnetic interaction between a coil and a magnet. This interaction depends on the excitation current signal (see Fig. 2) and the moment of magnetic forces:

$$T_{mag1} = M_{mag1} \cdot sgn(I_1),$$

$$T_{mag2} = M_{mag2} \cdot sgn(I_2). \tag{4}$$

During experiments, we observed an interesting phenomenon of a mutual excitation/synchronization of the magnets. When two pendulums are uncoupled and both equipped with the magnets, the magnetic fields of the magnets interact and create some "kind of connection" between the pendulums. Fig. 4 shows this phenomenon for a free swing of pendulum 2.

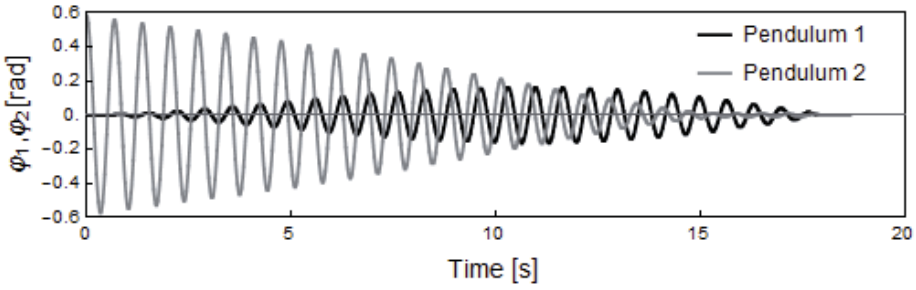

Figure 4. Interaction between pendulums with magnets.

It should be mentioned that though this phenomenon has been demonstrated experimentally, but it requires further experiments and simulations with two pendulums equipped with magnets due to lack of theoretical model of that interaction. This is why in this study we replaced the magnet in pendulum (1) with the brass element (in Eq. 1 we take $T_{mag1} = 0$).

The terms M_{mag1} and M_{mag2} represent the static characteristics of the magnetic forces reduced to the moment of force. The characteristics have been measured for pendulum 2. The way of measuring is schematically shown in Fig. 5.

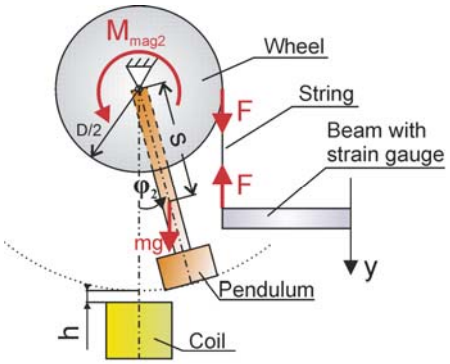

Figure 5. Method of measurement of the static characteristics of the magnetic forces.

The beam with strain gauge moves downward vertically with a constant velocity. The force F and the angle φ_2 are registered and processed by Eq. 5 to achieve

$$M_{mag2} = F \cdot \frac{D}{2} + mgs \cdot \sin\ \varphi_2, \tag{5}$$

where: F – measured force, D – diameter of the wheel.

The measurements have been carried out for two constant values of the coil current: $I_{a2} = 1\ A$ and $I_{a2} = 1.5\ A$. The obtained measurement points are shown in Fig. 6. Particular attention must be paid to the non-zero values of M_{mag2} for a zero angle achieved during the experiment. Though the fitted function should be multivalued for zero angle, however during modeling we have made an assumption that the moment of force is zero for zero angle because there is no moment arm. The experimental non-zero values of M_{mag2} for zero angle is yielded by not high enough resolution of the angle sensor.

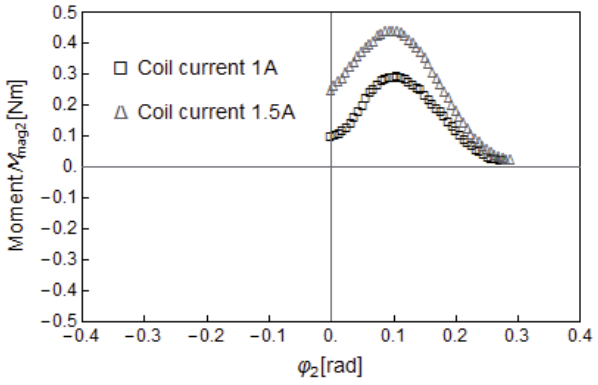

Figure 6. Experimental sets of points regarding the moment M_{mag2}

The obtained set of experimental points can be approximated by the following analytical formula

$$M_{mag2} = \mathrm{a} \cdot \mathrm{sgn}(\varphi) \cdot \exp\left[-\left(\frac{\mathrm{sgn}(\varphi)\cdot\varphi+b}{c}\right)^2\right], \tag{8}$$

where a, b, c are constant parameters being different for each possible values of the current.

It should be explained that the parameters a, b, c appeared in Eq. 8 influence M_{mag2}. Namely, the parameter a is responsible for extreme value of the function (8) for positive angles, whereas $(-b)$ is the argument for its extremum and c is responsible of its shape. For the negative angles, the values of M_{mag2} are symmetrical with respect to the positive angles. The fitted functions and symbolically illustrated a and $(-b)$ parameters are shown in Fig. 7.

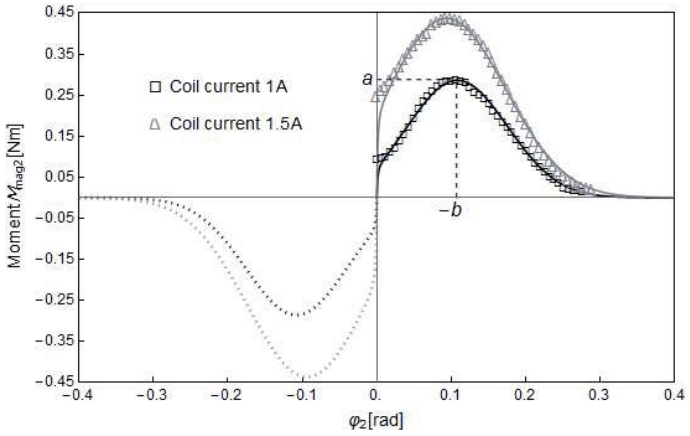

Figure 7. Experimental data versus the analytically approximated functions of the moment M_{mag2}.

4. Experiments versus numerical simulations

This section is aimed on the theoretical and experimental validation of the existence of regular and chaotic dynamics of our mechatronic system. Equations of motion (Eq. 1, 2) are solved numerically using the WOLFRAM MATHEMATICA software. For the purpose of effective simulations signum functions in Eqs. 3, 4 and 8 are replaced by $\frac{2}{\pi}\arctan(\epsilon \cdot x)$, where ϵ is large parameter [6]. That replacement causes that redefined functions and their first derivatives are continuous. The following parameters are fixed: $\epsilon = 10^3$, $I_1 = 6.8025 \cdot 10^{-4}\, kgm^2$, $I_2 = 6.7101 \cdot 10^{-4}\, kgm^2$, $mgs = 0.0578\, Nm$, $k_e = 2.532 \cdot 10^{-4}\, N/m$, $c_1 = 3.1 \cdot 10^{-5}\, Nms$, $c_2 = 7.2 \cdot 10^{-5} Nms$, $c_e = 13.736 \cdot 10^{-5} Nms$, $c_{B1} = 27.523 \cdot 10^{-5} Nm$, $c_{B2} = 27.888 \cdot 10^{-5} Nm$, $I_{a2} = 1A \rightarrow\ a = 0.287684, b = -0.107082, c = -0.095541$, $I_{a2} = 1.5A \rightarrow a = 0.439922, b = -0.092557, c = -0.112422$.

Fig. 8a shows simulation and experimental results of the free vibrations of uncoupled pendulums for the following initial conditions: $\varphi_1(0) = -1.56\, rad\ (-89.38°)$, $\varphi_2(0) = -0.025\, rad\ (-1.43°)$,

$\dot{\varphi}_1(0) = 0\frac{rad}{s}$ and $\dot{\varphi}_2(0) = 0\frac{rad}{s}$. Fig. 8b presents time histories of the numerically and experimentally obtained time histories of the excited coupled pendulums, where $I_{a2} = 1A$, $f = 2\ Hz, w = 25\%$. Initial conditions for simulations of the excited coupled pendulums are as follows: $\varphi_1(0) = 0\ rad$, $\varphi_2(0) = 1.75 \cdot 10^{-5}\ rad$ (0.001°), $\dot{\varphi}_1(0) = 0\ rad/s$ and $\dot{\varphi}_2(0) = 0\ rad/s$.

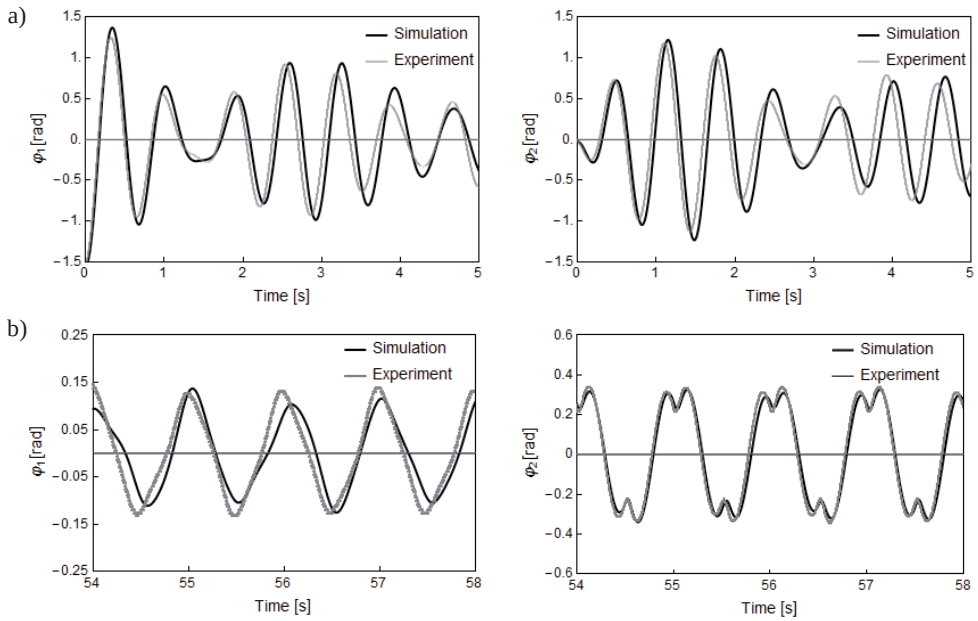

Figure 8. Comparison of simulation and experimental results: a) coupled pendulums – free vibrations, b) coupled pendulums with magnetically excited pendulum (2) ($I_{a2} = 1A, f = 2\ Hz, w = 25\%$).

In the case of regular vibrations, after omitting the transitional process, the coincidence of the numerical and experimental results is clearly visible.

However, the investigated system is very sensitive to small changes of the parameters like the duty cycle *w* and amplitude of the current. We have investigated the system experimentally for three different values of the duty cycle w: 27%, 30% and 33% when the current $I_{a2} = 1A$. We have also carried out the experiments for three amplitudes of the current I_{a2}: 0.5 A, 1 A, 1.5 A when the duty cycle $w = 30\%$. The results of the experiments are shown in the Fig. 9 in the form of bifurcation diagrams. The diagrams are made for increasing (→) frequency in a range 3.4-6 Hz. The system response for changes of the duty cycle plays a key role here. Taking into account Fig. $9a_2$ as a point of reference, one can say that a 3% increase in duty cycle results in significant reduction of chaotic area (represented by clusters of points) while preserving the period-2 motion. The 3% decrease in duty cycle leads to transition of period-2 motion into period-6 motion of the system. The influence of the

current changes is very similar to influence of the duty cycle. As it is seen in Fig. $9a_1$ and $9b_1$, the system motion type is similar and the frequency ranges are located closed to each other. Similarity of behavior has been also detected for the case of different current amplitude $I_{a2} = 1.5\ A$ (Fig. $9b_3$) and $I_{a2} = 1\ A$ (Fig. $9a_3$).

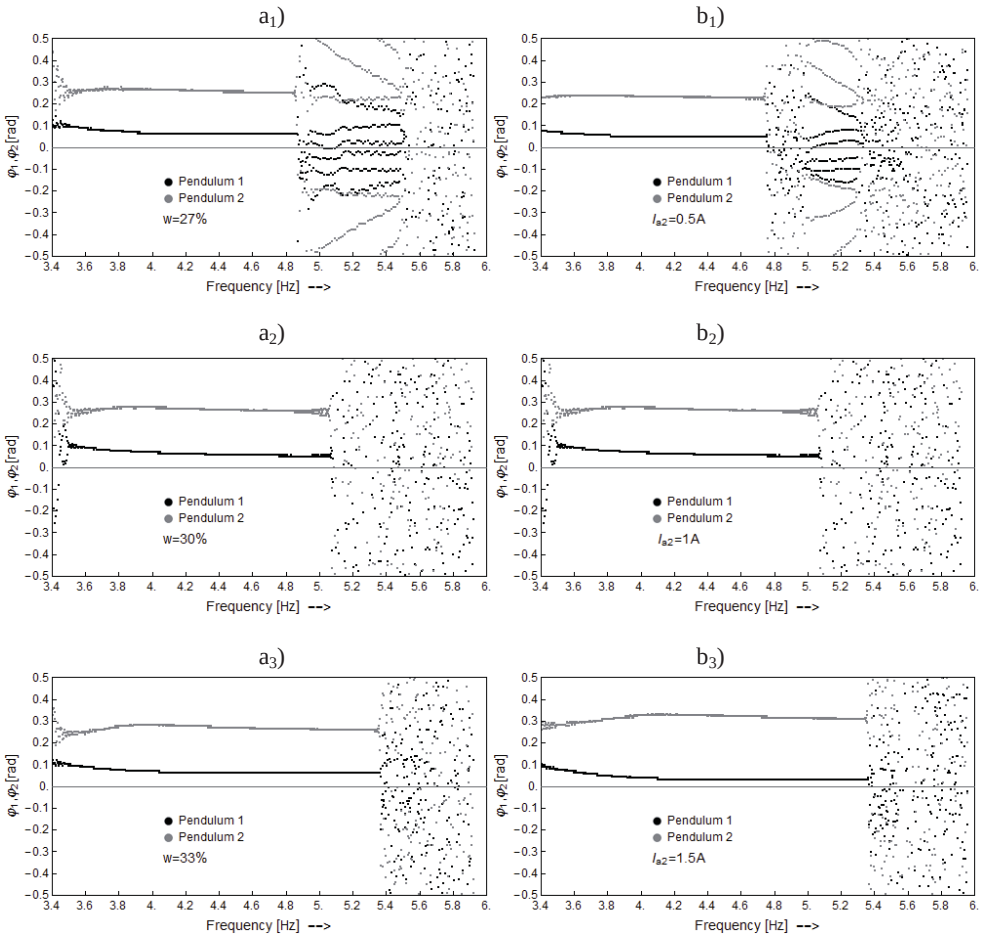

Figure 9. Experimental bifurcation diagrams for increasing frequency:
different duty cycles w for the current $I_{a2} = 1$A (a_1, a_2, a_3);
different amplitudes of the current for the duty cycle $w = 30\%$ (b_1, b_2, b_3).

Owing to the rich dynamics of the system responses we have chosen constant values of the current and duty cycle for a more detailed investigation of the motion. During our observations we have decided that parameters values $I_{a2} = 1A$ and $w = 30\%$ are optimal for thermal conditions of the coil. Our detailed investigation has been started by creating the bifurcation diagrams using numerical

simulations and then verifying them experimentally. The frequency range during simulation and experiment was 1.5-6 Hz. Experimental diagrams were done for linear increasing or decreasing frequency with average velocity $0.12\frac{Hz}{min}$. Figure 10 shows simulation and experiment results for pendulum 2 and for both frequency paths: increase (Fig. 10a, b) and decrease (Fig.10c, d). The simulation and experiment bifurcation diagrams coincide though the motion regions are slightly shifted. Differences between simulation and experiment diagrams can be explained by not sufficiently slow velocity of the frequency during the carried out experiment and by the discrepancies between model of the magnetic interaction and investigated approximation curve.

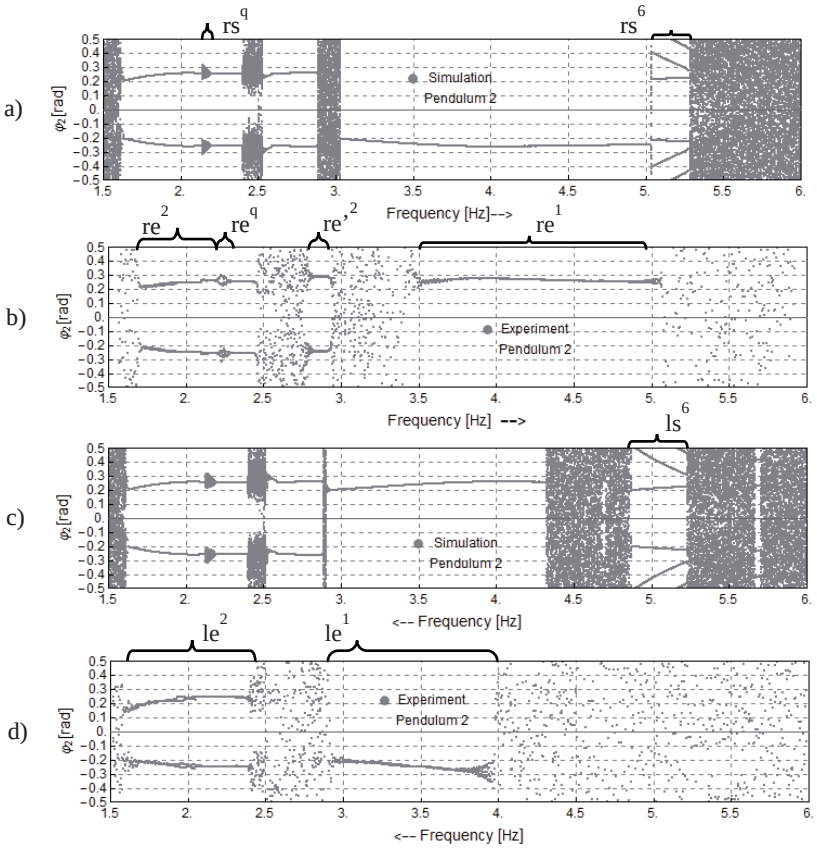

Figure 10. Experimental (laboratory) versus the numerically estimated bifurcation diagrams for the pendulum 2 ($I_{a2} = 1\ A, w = 30\%$).

We can see that direction of frequency path causes that some regions are mutually exclusive, and existence of regular dynamics in a region excludes chaotic behavior. At the same time, character of motion is the same for both pendulums. The system exhibits a few different types of regular motion

(examples labeled in Fig. 10): period-1 (re^1, le^1), period-2 (re^2, re'^2, le^2) and period-6 (rs^6, ls^6). The period-1 motion has two stable states for positive and negative angles (we can see that in both experimental and simulation bifurcation diagrams). The period-6 motion is not visible in experimental diagrams, however we have validated this character of motion after set the constant frequency on 5.1 Hz. Fig. 11 presents simulation and experimental results of the phase plane plots with the Poincaré sections for period-6 motion.

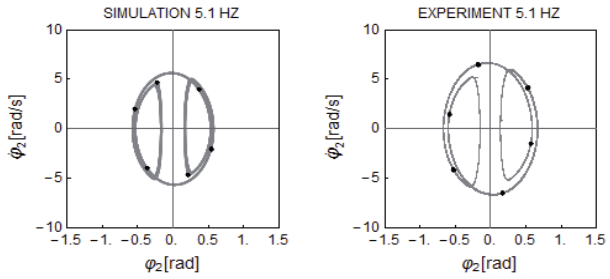

Figure 11. Phase plots with Poincaré sections for 5.1 Hz.

Period-1 and period-2 motions are confirmed by the phase 2D plots and the associated Poincaré maps, as shown in Figures 12, 13.

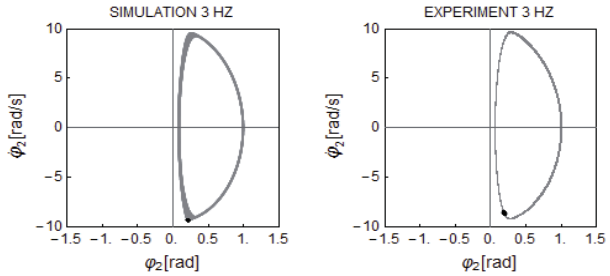

Figure 12. Phase plots with Poincaré sections of period-1 motion for 3 Hz.

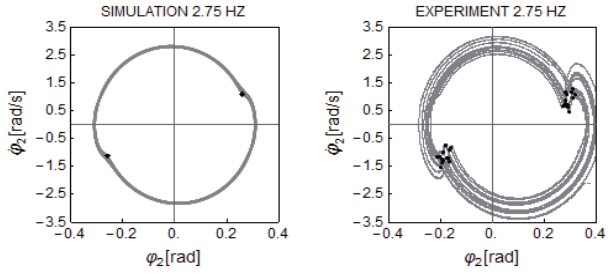

Figure 13. Phase plots with Poincaré sections of period-2 motion for 2.75 Hz

In particular, the sensitivity of the system on the initial conditions yields interesting results for region labeled rs^q (Fig. 10a) and corresponding to it region re^q (Fig. 10b). For earlier studied reasons, the above mentioned regions are shifted relative to each other. Therefore, for further investigations we take the fixed frequencies 2.17 Hz and 2.25 Hz corresponding to the middles of rs^q and re^q regions, respectively. Though in simulation we have achieved three different responses, but only one of them has been validated experimentally (see Fig. 14). Two of them are periodic: period-6 motion which has been observed during experiment (Fig. 14a), period-2 motion (Fig. 14b), whereas the third response presents quasi-periodic orbit (Fig. 14c). The employed initial conditions are as follows: period-2 → $\varphi_2(0) = 0.00052\, rad$ (0.03 °), $\varphi_1(0) = 0\, rad, \dot{\varphi}_1 = \dot{\varphi}_2 = 0\, rad/s$, period-6 → $\varphi_2(0) = 0.0012\, rad$ (0.07 °), $\varphi_1(0) = 0\, rad, \dot{\varphi}_1 = \dot{\varphi}_2 = 0\, rad/s$, quasi-periodicity → $\varphi_2(0) = 1.74 \cdot 10^{-5}\, rad$ (0.001 °), $\varphi_1(0) = 0\, rad, \dot{\varphi}_1 = \dot{\varphi}_2 = 0\, rad/s$.

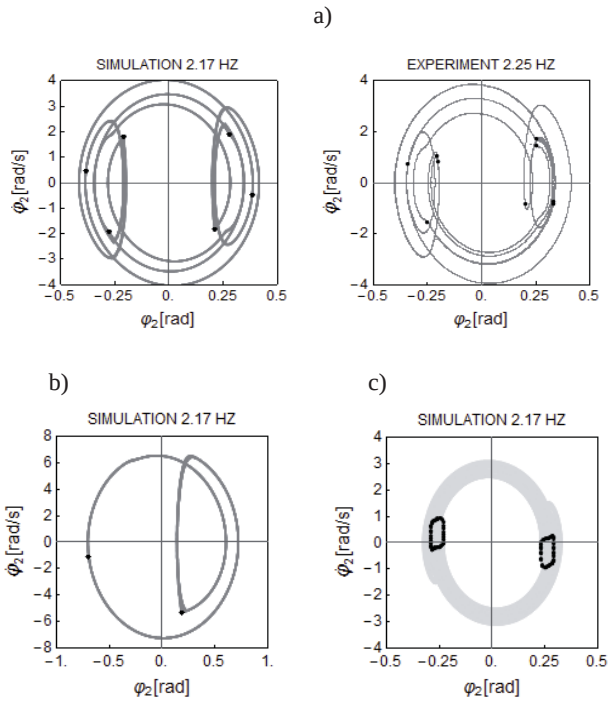

Figure 14. Phase portraits with Poincaré sections for the region rs^q and the corresponding re^q for different initial conditions: a) period-6 motion; b) period-2 motion; c) quasi-periodic motion.

5. Conclusion

The studied system of two pendulums coupled elastically and driven by the magnetic field exhibited rich non-linear dynamical behaviour. We have found numerically and proved experimentally the existence of regular and chaotic motion of the system. We have constructed the bifurcation diagrams,

phase portraits with Poincaré sections by using numerical simulations, and we have validated them experimentally. The simulation results show good agreement with the experimental results. We can observe sensitivity of the system to initial conditions and different values of the control parameters (frequency, amplitude of coil current, duty cycle). Our physical model may serve as a good starting point for modelling of electric motors like steeper motors, which have flexible shaft or are joined through an elastic clutch. It should be mentioned that the influence of control parameters to the system behaviour is not fully examined in this paper, and it stands for further studies. Furthermore, the mathematical model of magnetic interaction also requires a detailed study.

References

[1] Siahmakoun, A., French, V., and Patterson, J. Nonlinear dynamics of a sinusoidally driven pendulum in a repulsive magnetic field. *American Journal of Physics* 65, 393 (1997), 393-400.

[2] Kraftmakher, Y. Demonstrations with a magnetically controlled pendulum. *American Journal of Physics* 78, 532 (2010), 532-535.

[3] Khomeriki, G. Parametric resonance induced chaos in magnetic damped driven pendulum. *Physics Letters A* 380 (2016), 2382–2385.

[4] Tran, V., Brost, E., Johnston, M., and Jalkiod, J. Predicting the behavior of a chaotic pendulum with a variable interaction potential. *Chaos* 23, 033103 (2013), 12 pp.

[5] Griffiths, D. J. *Introduction to Electrodynamics*. Prentice-Hall, New Jersey, 1999.

[6] Wasilewski, G., Kudra, G., Awrejcewicz, J., Kaźmierczak, M., Tyborowski, M., and Kaźmierczak M. Experimental and numerical investigations of a pendulum driven by a low-powered DC motor, in: Awrejcewicz J., Kaźmierczak M., Olejnik P. and Mrozowski J. (eds.) *Dynamical Systems—Mathematical and Numerical Approaches*, TU of Lodz, Lodz, 2015, pp. 579–590.

Krystian Polczyński, B.A. (M.Sc. student): Lodz University of Technology, Faculty of Mechanical Engineering, Department of Automation, Biomechanics and Mechatronics, Stefanowskiego 1/15, 90-924, Lodz, POLAND (*kryst.polczynski@gmail.com*).

Grzegorz Wasilewski, Ph.D.: Lodz University of Technology, Faculty of Mechanical Engineering, Department of Automation, Biomechanics and Mechatronics, Łąkowa 19/21, POLSKA (*grzegorz.wasilewski@p.lodz.pl*).

Jan Awrejcewicz, Professor: Lodz University of Technology, Faculty of Mechanical Engineering, Department of Automation, Biomechanics and Mechatronics, Stefanowskiego 1/15, 90-924, Lodz, POLAND (*jan.awrejcewicz@p.lodz.pl*).

Adam Wijata, M.Sc. (Ph.D. student): Lodz University of Technology, Faculty of Mechanical Engineering, Department of Automation, Biomechanics and Mechatronics, Stefanowskiego 1/15, 90-924, Lodz, POLAND (*adam.wijata@dokt.p.lodz.pl*).